



Published in final edited form as:

Biomater Sci. 2019 August 01; 7(8): 3138–3142. doi:10.1039/c9bm00785g.

Delivery of siRNA therapeutics using cowpea chlorotic mottle virus-like particles

Patricia Lam^{a,\$}, Nicole F. Steinmetz^{a,b,*}

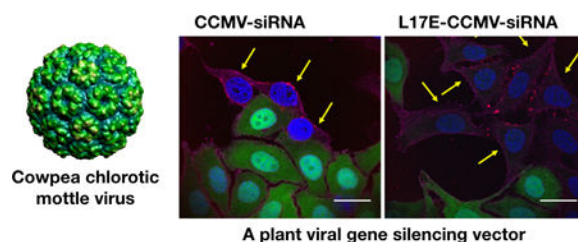
^a.Department of Biomedical Engineering, Case Western Reserve University, Cleveland OH 44106.

^b.Departments of NanoEngineering, Bioengineering, Radiology, Moores Cancer Center, University of California San Diego, La Jolla 92093.

Abstract

While highly promising in medicine, gene therapy requires delivery agents to protect and target nucleic acid therapeutics. We developed a plant viral siRNA delivery platform making use of self-assembling cowpea chlorotic mottle virus (CCMV). CCMV was loaded with siRNAs targeting GFP or FOXA1; to further enhance cell uptake and intracellular trafficking, resulting in more efficient gene knockdown, we appended CCMV with a cell penetrating peptide (CPP), specifically M-lycotoxin peptide L17E.

Graphical Abstract



Nucleic acid therapeutics have wide ranging applications: DNA or RNA coding for functional proteins and enzymes could overcome loss-of function mutations and thus provide hope for patients with genetic disorders such as cystic fibrosis ¹ and muscular dystrophy ². Other avenues focus on delivery of small regulatory RNAs, such as small interfering RNAs (siRNAs), microRNAs (miRNAs), as well as anti-miRs to regulate protein expression ³. Gene silencing with siRNA holds tremendous promise in cancer therapy and beyond; synthetic siRNAs can be designed to target in principle any gene of interest ⁴, therefore enabling downregulation of genes involved in cell proliferation, epithelial-mesenchymal transition, or drug resistance. Several strategies are in clinical testing ⁵.

* nsteinmetz@ucsd.edu.

\$Current address: Center for Gene Therapy, The Research Institute at Nationwide Children's Hospital, Columbus OH 43205

Electronic Supplementary Information (ESI) available: Materials and Methods. See DOI: [10.1039/x0xx00000x](https://doi.org/10.1039/x0xx00000x)

Conflicts of interest

There are no conflicts to declare.

However, to make a clinical impact, a delivery strategy is required, because ‘naked’ siRNAs are not stable in plasma, not targeted, and their negative charge impairs efficient cell uptake.

Many different delivery platforms have been proposed, all of which have their advantages and disadvantages. One principally differentiates viral vs. non-viral delivery systems. Several mammalian viruses, such as lentivirus and adeno-associated virus (AAV) have been developed for gene therapy⁶. Because viruses have evolved machinery and mechanism to navigate cell trafficking, these systems are highly efficient⁷. However drawbacks are possible adverse effects as a result gene integration⁸ and their inherent immunogenicity⁹. Also, a library of non-viral delivery systems has been explored¹⁰. While non-viral systems generally do not match the effectiveness of viral delivery systems, these systems offer safety. Technological challenges can be instability in biological media leading to aggregation and/or premature cargo release^{11, 12}. While several highly sophisticated systems have been reported in recent years^{13–15}, there is a continued need for the development of efficient gene delivery vehicles. Toward this goal, we have turned toward the study of plant viruses as an intermediate between the viral and non-viral delivery system.

Plant viruses offer an exciting platform nanotechnology for several reasons: plant viruses are non-infectious toward mammals¹⁶, with no apparent toxicities observed at doses up to 100 mg/kg^{17, 18}. While ‘naked’ plant viruses are immunogenic, we have shown that stealth^{19, 20} or ‘self’ coatings reduce immunogenicity and enable evasion from carrier-specific antibodies²¹. Lastly molecular farming in plants is cost-effective and high yielding²². Compared to the non-viral counterparts, (plant) viruses provide monodisperse nanoparticle preparations, thus offering a high degree of quality control and assurance; and being biological materials, (plant) viruses show exceptional stability in biological media²³.

Plant viruses are being developed for diverse applications in drug delivery²⁴; however, to date there is only few examples of their use as gene delivery vectors. Principally, tobacco mosaic virus (TMV) and cowpea chlorotic mottle virus (CCMV) have been tested for gene therapy. TMV was engineered to deliver mRNA for vaccine applications²⁵. Further, proof-of-concept of CCMV-mediated gene delivery has been established using CCMV delivering heterologous mRNA encoding for green fluorescent protein (GFP). Here the RNA cargo was stabilized through encapsulation into the plant viral capsid and released into the cytoplasm of mammalian cells facilitating protein expression, however this was only achieved through co-delivery with Lipofectamine-2000²⁶.

In this work, we established the application of CCMV to deliver siRNAs targeting first GFP for proof of concept and the forkhead box transcription factor (FOXA1) as a therapeutic target²⁷. To mediate cell trafficking and overcome the need for use of Lipofectamine, we appended CCMV with cell penetrating peptides (CPPs), specifically M-lycotoxin peptide L17E²⁸.

CCMV particles were produced in black-eyes peas No. 5 by mechanical inoculation and purification from homogenized leaves by chloroform extraction, PEG precipitation, and ultracentrifugation; as an alternative, we also produced CCMV coat proteins using an *E. coli* expression system (both methods are described in detail in the Supplementary Information).

First, we established whether CCMV would enter mammalian cells using HeLa cells, a well-established cancer cell line. For imaging and flow cytometry analysis, Cyanine5 (Cy5)-labeled CCMV was obtained using an NHS-activated Cy5 enabling coupling to CCMV's surface lysines²⁹ (Supplementary Information). UV/vis spectroscopy indicated that CCMV was labeled with approximately 60 Cy5 dyes per CCMV particle.

For quantitative flow cytometry assays, 1×10^5 CCMV per cell were added and particles were allowed to interact with HeLa cells for 6 hours. Cells were treated with pronase to assess the level of surface-bound CCMV. Similarly, confocal microscopy studies were performed; flow cytometry and imaging data are in agreement and indicate that CCMV indeed enters HeLa cells; only a fraction of particles remain surface bound and hence are removed by the pronase treatment (Figure 1A+B). Significant co-localization with cell surface marker wheat germ agglutinin (WGA) was not observed; however, staining with an endolysosomal marker (Lamp-1) revealed that CCMV is partially entrapped within endolysosomal vesicles (Manders coefficient of $M_{\text{CCMV}} \text{ vs. } LAMP-1 = 0.32$, Figure 1C+D); i.e. data suggest that CCMV at least partially escapes the endolysosomal compartment. Based on these encouraging data, we prepared siRNA-laden CCMV with and without CPP L17E.

siRNA encapsulation was achieved making use of well-established, pH- and salt-controlled, dis- and assembly methods³⁰; to yield CCMV loaded with siRNA, the dicer substrate siRNA as well as their non-targeted control RNAs were added at a 6:1 (w/w) ratio (Figure 2A; see Supplementary Information). Transmission electron microscopy (TEM) imaging revealed that reconstituted CCMV carrying siRNAs were structurally sound forming 30 nm-sized icosahedral particles (Figure 2B,C).

Next, a CPP was added; specifically, we chose the M-lycotoxin peptide L17E²⁸. This peptide was initially derived from spider venom; the L17E has Glu additions to reduce the overall positive charge and therefore enhance function. Data suggest that the L17E preferentially disrupts endolysosomal over plasma membranes; furthermore, when added to biologics (such as antibodies), L17E promotes cell uptake by micropinocytosis, thus making it a promising candidate for nanoparticle-mediated gene delivery. We reasoned that the addition of the CPP would be beneficial and increase efficacy of siRNA delivery, because our data showed that CCMV, at least in part, is entrapped in the endolysosomal compartment (see Figure 1).

The following peptide was synthesized: IWLTKFLGKHAACKHEAKQQLSKL with C-terminal amide or Gly-Gly-Cys linker; the latter was used for bioconjugation to CCMV's surface lysines using an SM(PEG)₄ linker (detailed protocols are listed in the Supplementary Information). Varying the peptide:CCMV ratio did not have significant impact on the labeling efficiency. SDS-PAGE revealed that ~ 15–20% of CCMV's coat proteins were modified using molar ratios of 600, 900, and 1200:1 peptide:CCMV (Figure 2D); or in other words, the conjugation yielded CCMV displaying ~ 30 L17E peptides per particle (Figure 2D). Quantification was carried out by measuring the band density comparing L17E-labeled CP vs. native CP using band analysis tool and ImageJ software. Using these methods, we then produced dual-functional CCMV loaded with siRNA and tagged with L17E peptides (Figure 2E); SDS-PAGE revealed successful conjugation of the CPP, and agarose gel

electrophoresis using a nucleic acid stain revealed successful encapsulation of the siRNA cargo (Figure 2F). Using a fluorescently-labeled eGFP-Cy3 siRNA we determined that CCMV could encapsulate 2–3 μ M siRNAs (detailed methods are described in the Supplementary Information).

First, for proof-of-concept, we used GFP-expressing HeLa cells and treated these with siRNA-loaded CCMV particles with and without L17E peptide; control experiments included the use of free siRNA and CCMV-delivered siRNA in combination with lipofectamine; we used target and non-target siRNAs (at a 7.5–10 nM concentration; Supplementary Information). Confocal microscopy revealed successful gene silencing mediated by the plant viral siRNA delivery vector (Figure 3A–F): comparing siRNA-loaded CCMV vs. CCMV-L17E it was apparent that the addition of the L17E peptide increased efficacy; GFP expression was silenced across more cells. For either nanoparticle formulation it was apparent that GFP silencing was not achieved uniformly across all cells; however, cells that showed positive signals for CCMV (shown in red in Figure 3), loss of GFP fluorescence was apparent (Figure 3B+C). Quantitative analysis using real time qPCR (detailed methods are listed in the Supplementary Information) showed that indeed addition of the L17E CPP increased the effectiveness of the gene silencing approach; while CCMV alone yielded 30% downregulation of GFP expression, the siRNA-loaded L17E-CCMV formulation achieved 50% downregulation of GFP mRNA. Interestingly, mixing CCMV with the L17E peptide did not give rise to gene silencing (sample: L17E+CCMV-siRNA). A previous study showed that physical mixtures of the L17E peptide and antibodies enabled cytosolic delivery of therapeutic antibodies²⁸. In contrast, L17E + CCMV mixtures resulted in aggregation, likely based on the polyvalent nature of the CCMV particles with its overall negative surface charge building multi-particle interlinkages with the positively-charged L17E peptide (pI ~ 10); therefore, preventing cell uptake, cargo delivery, and gene silencing (Figure 3G).

Lastly, we selected siRNAs to target FOXA1 as a potential therapeutic target in breast cancer²⁷ or prostate cancer. Data indicate a critical role of FOXA1 in cell proliferation, and studies suggest that gene silencing is indeed a successful strategy to inhibit cell proliferation and induce G0/G1 arrest³¹. Here we tested whether CCMV formulated with siRNAs targeting FOXA1 would allow gene silencing using the breast cancer cell line MCF-7. Data indicate that siRNA-loaded CCMV alone was not effective in silencing the target gene FOXA1; however, conjugation of the CPP L17E restored efficacy leading to knockdown of FOXA1 mRNA levels by ~ 50%, matching the effectiveness of lipofectamine (Figure 4). However, also here we found that the L17E peptide needed to be covalently conjugated and displayed on CCMV; physical mixtures of siRNA-loaded CCMV + L17E peptide had no efficacy, which again can be explained by instability of this mixture.

Conclusions

We demonstrate that siRNA molecules can be effectively loaded into CCMV nanoparticles. While target gene knockdown using the native CCMV protein was observed using HeLa cells overexpressing GFP, only CCMV with appended CPPs, here M-lycotoxin peptide L17E, were efficient in silencing FOXA1 gene. While plant viruses offer advantageous

properties for biological applications, they have not evolved the sophisticated machinery of mammalian viral vectors, to navigate the cellular compartments of mammalian cells. Therefore, the addition of CPPs or other strategies that would prime endolysosomal escape likely will be beneficial for the development of effective plant viral gene delivery vectors. Similar observations have been made using the capsids from bacteriophages^{32, 33}, which, like plant viruses, offer a highly intriguing nanotechnology platform but lack mechanism to engage with mammalian cells. Nevertheless, gene silencing using the native CCMV capsid was apparent and imaging data indicate that the CCMV nanoparticle was only partially trapped within the endolysosomal compartment. In conclusion, this study lays a foundation for the use of CCMV for siRNA delivery.

Supplementary Material

Refer to Web version on PubMed Central for supplementary material.

Acknowledgments

This work was funded in part by a grant from the NIH CA224605.

Notes and references

1. Cooney AL, McCray PB Jr. and Sinn PL, *Genes (Basel)*, 2018, 9, 538.
2. Duan D, *Mol Ther*, 2018, 26, 2337–2356. [PubMed: 30093306]
3. Mowa MB, Crowther C, Ely A and Arbuthnot P, *Biomed. Res. Int*, 2014, 2014, 718743. [PubMed: 25003129]
4. Tatiparti K, Sau S, Kashaw SK and Iyer AK, *Nanomaterials (Basel)*, 2017, 7, 77.
5. Sridharan K and Gogtay NJ, *Br J Clin Pharmacol*, 2016, 82, 659–672. [PubMed: 27111518]
6. Lundstrom K, *Diseases*, 2018, 6, 42.
7. Anderson WF, *Nature*, 1998, 392, 25–30.
8. Couzin J and Kaiser J, *Science*, 2005, 307, 1028.
9. Verma IM, *Mol. Ther*, 2000, 2, 415–416. [PubMed: 11082313]
10. Yin H, Kanasty RL, Eltoukhy AA, Vegas AJ, Dorkin JR and Anderson DG, *Nat Rev Genet*, 2014, 15, 541–555. [PubMed: 25022906]
11. Wiethoff CM and Middaugh CR, *J Pharm Sci*, 2003, 92, 203–217. [PubMed: 12532370]
12. Kwok DY, Coffin CC, Lollo CP, Jovenal J, Banaszczyk MG, Mullen P, Phillips A, Amini A, Fabrycki J, Bartholomew RM, Brostoff SW and Carlo DJ, *Biochim Biophys Acta*, 1999, 1444, 171–190. [PubMed: 10023051]
13. Zhou D, Cutlar L, Gao Y, Wang W, O’Keeffe-Ahern J, McMahon S, Duarte B, Larcher F, Rodriguez BJ, Greiser U and Wang W, *Sci Adv*, 2016, 2, e1600102. [PubMed: 27386572]
14. Liu S, Zhou D, Yang J, Zhou H, Chen J and Guo T, *J Am Chem Soc*, 2017, 139, 5102–5109. [PubMed: 28322564]
15. Zeng M, Zhou D, Alshehri F, Lara-Saez I, Lyu Y, Creagh-Flynn J, Xu Q, Zhang SA, J and Wang W, *Nano Lett*, 2019, 19, 381–391. [PubMed: 30565945]
16. Manchester M and Singh P, *Adv Drug Deliv Rev*, 2006, 58, 1505–1522. [PubMed: 17118484]
17. Kaiser CR, Flenniken ML, Gillitzer E, Harmsen AL, Harmsen AG, Jutila MA, Douglas T and Young MJ, *Int J Nanomedicine*, 2007, 2, 715–733. [PubMed: 18203438]
18. Singh P, Prasuhn D, Yeh RM, Destito G, Rae CS, Osborn K, Finn MG and Manchester M, *J Control Release*, 2007, 120, 41–50. [PubMed: 17512998]

19. Lee KL, Shukla S, Wu M, Ayat NR, El Sanadi CE, Wen AM, Edelbrock JF, Pokorski JK, Commandeur U, Dubyak GR and Steinmetz NF, *Acta Biomater*, 2015, 19, 166–179. [PubMed: 25769228]
20. Bruckman MA, Randolph LN, Gulati NM, Stewart PL and Steinmetz NF, *J Mater Chem B Mater Biol Med*, 2015, 3, 7503–7510. [PubMed: 26659591]
21. Gulati NM, Pitek AS, Czapar AE, Stewart PL and Steinmetz NF, *J. Mater. Chem. B*, 2018, 6, 2204–2216 [PubMed: 30294445]
22. Schneemann A and Young MJ, *Adv Protein Chem*, 2003, 64, 1–36. [PubMed: 13677044]
23. Pitek AS, Wen AM, Shukla S and Steinmetz NF, *Small*, 2016, 12, 1758–1769. [PubMed: 26853911]
24. Sokullu E, Soleymani Abyaneh H and Gauthier MA, *Pharmaceutics*, 2019, 11, 211.
25. Zhou Y, Maharaj PD, Mallajosyula JK, McCormick AA and Kearney CM, *Mol Biotechnol*, 2015, 57, 325–336. [PubMed: 25432792]
26. Azizgolshani O, Garmann RF, Cadena-Nava R, Knobler CM and Gelbart WM, *Virology*, 2013, 441, 12–17. [PubMed: 23608360]
27. Bernardo GM, Bebek G, Ginther CL, Sizemore ST, Lozada KL, Miedler JD, Anderson LA, Godwin AK, Abdul-Karim FW, Slamon DJ and Keri RA, *Oncogene*, 2013, 32, 554–563. [PubMed: 22391567]
28. Akishiba M, Takeuchi T, Kawaguchi Y, Sakamoto K, Yu HH, Nakase I, Takatani-Nakase T, Madani F, Graslund A and Futaki S, *Nat Chem*, 2017, 9, 751–761. [PubMed: 28754944]
29. Gillitzer E, Willits D, Young M and Douglas T, *Chem Comm*, 2002, 2390–2391. [PubMed: 12430455]
30. Comas-Garcia M, Garmann RF, Singaram SW, Ben-Shaul A, Knobler CM and Gelbart WM, *J Phys Chem B*, 2014, 118, 7510–7519. [PubMed: 24933579]
31. Imamura Y, Sakamoto S, Endo T, Utsumi T, Fuse M, Suyama T, Kawamura K, Imamoto T, Yano K, Uzawa K, Nihei N, Suzuki H, Mizokami A, Ueda T, Seki N, Tanzawa H and Ichikawa T, *PLoS One*, 2012, 7, e42456. [PubMed: 22879989]
32. Wei B, Wei Y, Zhang K, Wang J, Xu R, Zhan S, Lin G, Wang W, Liu M, Wang L, Zhang R and Li J, *Biomed Pharmacother*, 2009, 63, 313–318. [PubMed: 18823738]
33. Galaway FA and Stockley PG, *Mol Pharm*, 2013, 10, 59–68. [PubMed: 23110441]

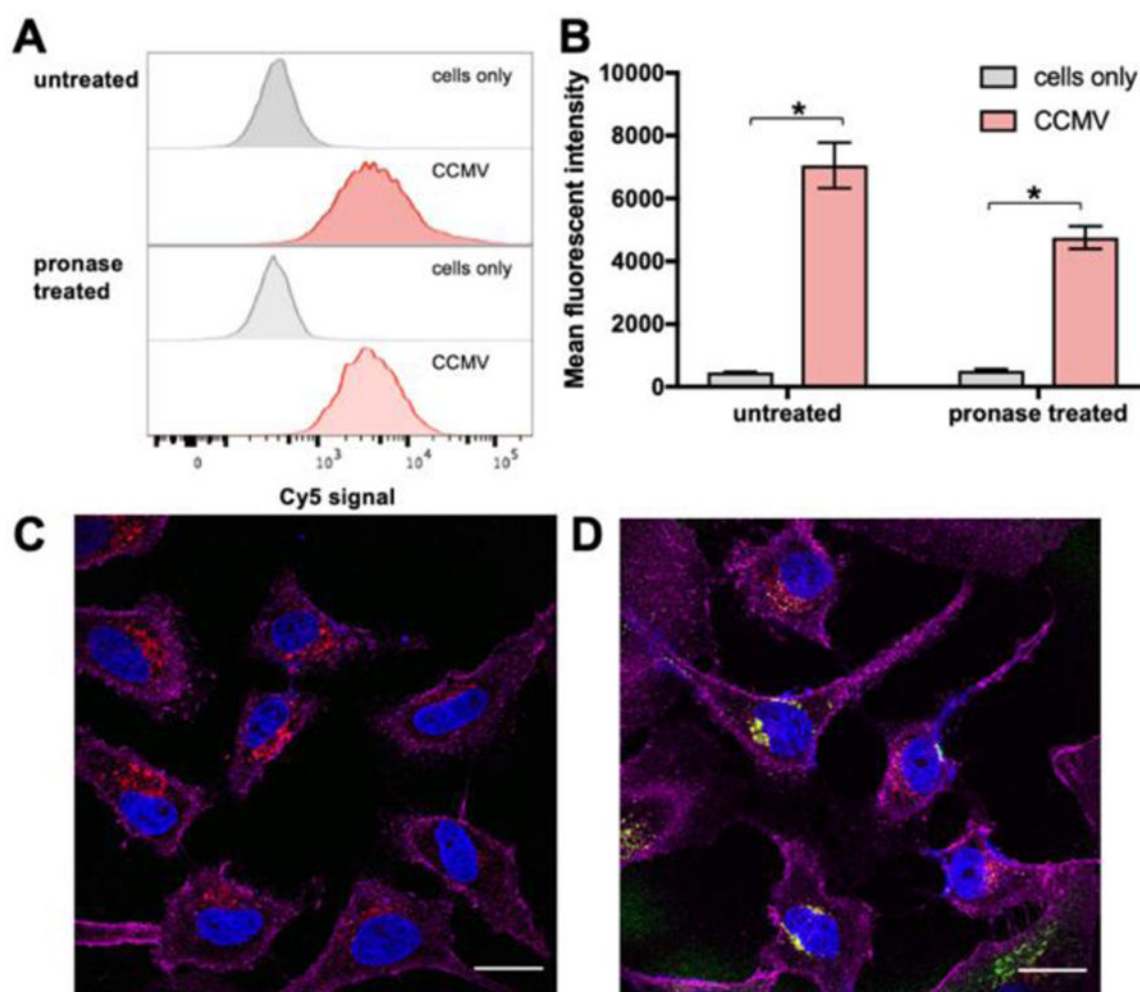


Figure 1.

(A) Flow cytometry was used to assess the uptake of CCMV-Cy5 in HeLa cells after incubation at 37°C for 6h. Following incubation, cells were treated with and without pronase to remove any loosely bound particles from the cell. (B) mean fluorescence intensity. (C,D) Confocal microscopy of HeLa cells (C), and HeLa cells with CCMV-Cy5 particles (D). DAPI in blue; LAMP1 (lysosomes) in red; WGA (membrane) in magenta; CCMV particles in green. Scale bar = 25 μ m.

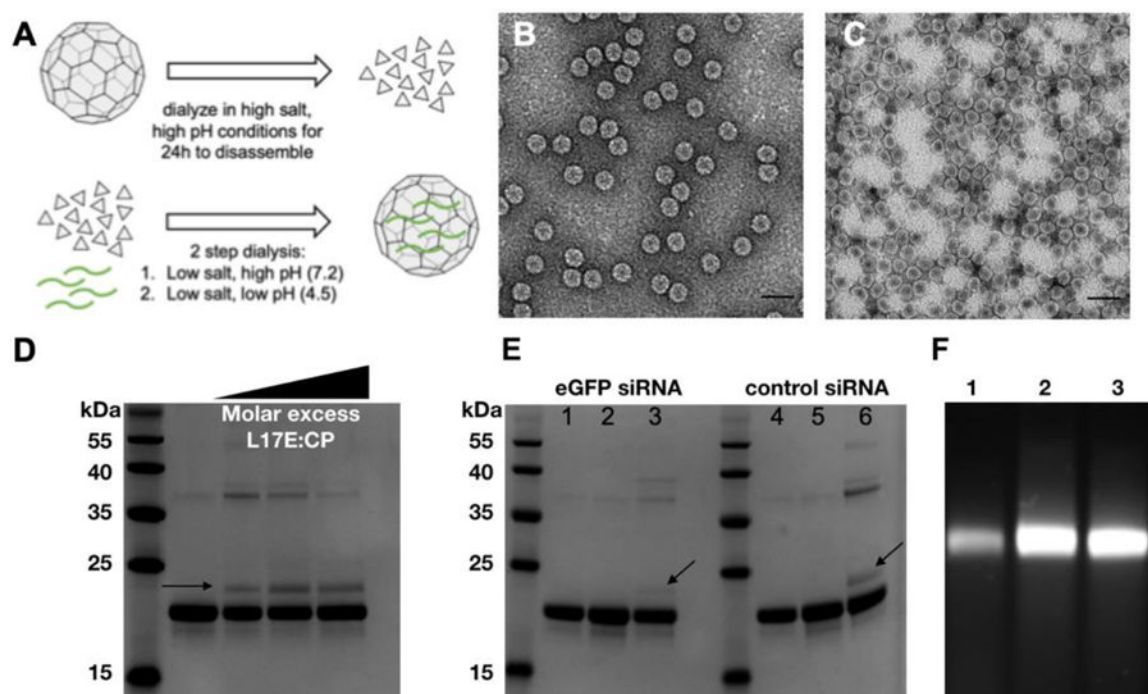


Figure 2.

Characterization of reassembled CCMV particles. (A) Scheme for disassembly of whole CCMV virions to coat proteins, then the reassembly around heterologous siRNAs to make CCMV-siRNA. (B) Transmission electron micrograph of CCMV particles. (C) Transmission electron micrograph of reassembled CCMV particles. Scale bar = 50 nm. (D) SDS-PAGE analysis of CCMV after conjugation with various molar excesses (600, 900, 1200:1 L17E:CCMV) of the cell penetrating peptide m-lycotoxin, L17E (CPP). The CCMV single coat protein is approximately 20 kDa. Successful conjugation is indicated by the higher molecular weight band (see arrow). (E) SDS-PAGE analysis of reassembled CCMV encapsulated eGFP siRNA or negative control siRNA. Lanes 1, 4 = CCMV; 2, 5 = reassembled CCMV; 3, 6 = reassembled L17E-labeled CCMV. (F) Agarose gel electrophoresis showing successful encapsulation of siRNA in reassembled CCMV. Lane 1 = CCMV (positive control); 2 = CCMV-eGFPsiRNA; 3 = CCMV-neg-siRNA.

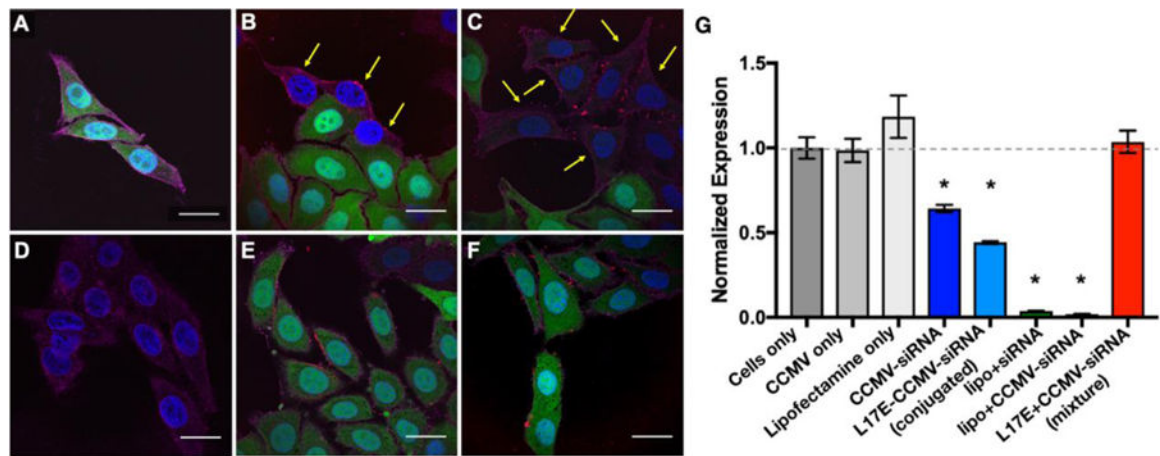


Figure 3.

siRNA silencing of HeLa/GFP cells. (A-F) Confocal microscopy of HeLa/GFP cells treated with different particle formulations for 24 hours. Loss of eGFP expression occurred when cells were treated with siRNA targeting eGFP. (A) HeLa/GFP cells only control. (B-C) Cells treated with CCMV-eGFPsiRNA and CCMV-mlyco-eGFPsiRNA (mlyco=L17E peptide), respectively. CCMV particles (red) are present in cells with no eGFP expression. (D) Cells treated with lipofectamine+eGFPsiRNA; (E-F) with CCMV-negsiRNA and CCMV-mlyco-negsiRNA. Particles are visible in the cell indicating cell uptake, but no silencing of eGFP present. DAPI in blue; CCMV particles in red; WGA (membrane) in magenta; HeLa/GFP cells in green. Scale bar = 25µm. (G) Quantitative real-time PCR showing relative levels of eGFP expression in cells after various treatments. Statistically significant changes in eGFP expression relative to the cells only control after a one-way ANOVA are indicated with *.

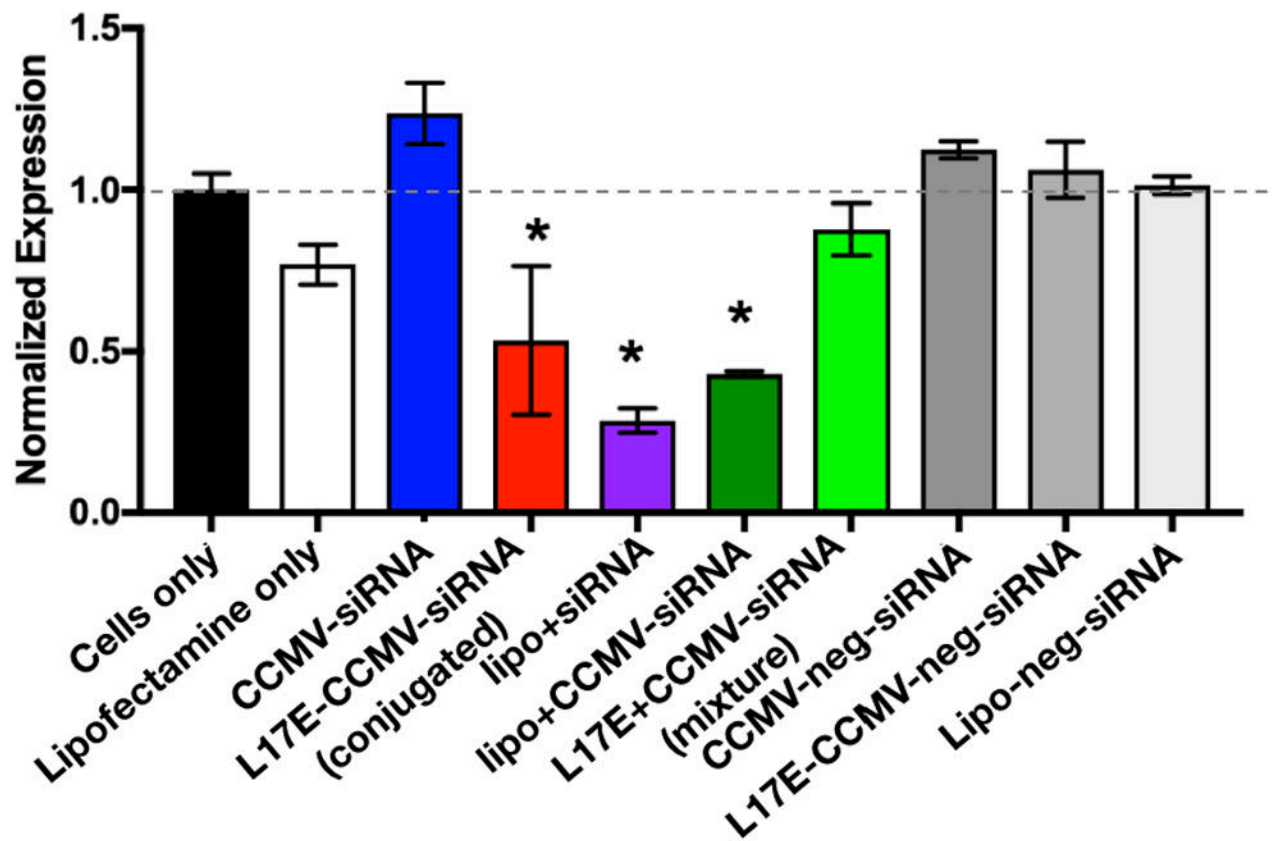


Figure 4.

Quantitative real time PCR assessing the level of FOXA1 expression in MCF-7 cells after treatment with siRNAs, delivered with lipofectamine or encapsulated within CCMV and CCMV conjugated with m-lycotoxin L17E peptide (CPP). Statistically significant changes in FOXA1 expression relative to the cells only control after a one-way ANOVA are indicated with *.